Int. J. Electrochem. Sci., 11 **(2016)** 4219 – 4230, doi: 10.20964/2016.06.25

International Journal of ELECTROCHEMICAL SCIENCE
www.electrochemsci.org

Test of Different Anode Electrocatalysts for Direct Glucose Anion Exchange Membrane Fuel Cell

Spets Jukka-Pekka[1,*], *Kanninen Petri*[2], *Kallio Tanja*[2], *Selkäinaho Jorma*[3], *Kiros Yohannes*[4], *Saari Kari*[1], *Larmi Martti*[1]

[1] Dept. Mechanical Engineering, School of Engineering, Aalto University, Espoo, P.O. Box 14400, FI-00076 Aalto, Finland
[2] Dept. Chemistry, School of Chemical Technology, Aalto University, Espoo, P.O. Box 16000, FI-00076 Aalto, Finland
[3] Dept.Electrical Engineering and Automation, School of Electrical Engineering, Aalto University, Espoo, P.O. Box 15500, FI-00076 Aalto, Finland
[4] Dept. Chemical Engineering and Technology, KTH – Royal Institute of Technology, SE-100 44 Stockholm, Sweden
[*]E-mail: jukka-pekka.spets@aalto.fi

Received: 3 March 2016 / *Accepted:* 23 March 2016 / *Published:* 4 May 2016

Direct glucose anion exchange membrane fuel cell (AEMFC) with near-neutral-state electrolyte of 0.1 M $[PO_4]_{tot}$ was studied with five different anode electrocatalysts (Pt, PtRu, PtNi, Au, PdAu) at a temperature of 37 ^oC and at a glucose concentration of 0.1 M. The cathode catalyst in each test was Pt supported on carbon (60 wt.%). Four anode electrocatalysts (supported on carbon) had a total metal content of 40 wt.% while the fifth anode material of PtRu had a higher content of 60 wt.%. Moreover, in order to show the influence of the metallic content on the fuel cell performance, anode catalysts with 60 wt.% (Pt) and 10wt.% (PtNi) were tested. The operation of the AEMFC was controlled by means of an in-house-made electronic load with PI-controller (i.e. a feedback controller that has proportional and integral action on control error signal) either at constant current (CC) or at constant voltage (CV). The primary objective was to characterize the Coulombic efficiency (CE) based on the exchange of two electrons and compare the specific energy (Wh kg^{-1}) for the direct glucose AEMFC related to the different electrode combinations and electrocatalysts. As a result of these screening tests, two most efficient anode electrodes with Pt and PtNi were selected to be used for further AEMFC studies.

Keywords: glucose, anode electrocatalysts, anion exchange membrane fuel cell, near-neutral-state electrolyte

1. INTRODUCTION

Monosaccharide glucose is an attractive and ecological fuel for the direct fuel cells [1]. Different abiotic and microbial direct glucose fuel cells have been under intense research and

development in recent years [2-6]. A lot of unsuccessful work has been carried out since then to reproduce the impressive results of extracting 17.5 e^- per glucose molecule within 800 hours at pH 7.4 in the direct glucose fuel cell as reported by Richter et al. [2-3]. In these tests the diffusion of oxygen from the cathode side to the anode was prevented by membrane structure for the implantable fuel cell type [2-3]. Recently published electron yields have been mainly maximum two electrons of the available 24 electrons per glucose molecule in the direct fuel cells either with near-neutral-state or alkaline electrolytes [4,7]. The difference can be explained by the use catalysts by Richter et al. [2-3], which might decrease unwanted side reactions as the oxidation of glucose is kinetically limited. When compared to other reported results with microbial fuel cells [8], the corresponding redox reactions of biological compounds (i.e. NADH) occur with slow reaction rates giving rise to low current densities.

In this study, we report the test of different catalysts for the oxidation of glucose for application in AEMFC. A glucose concentration of 0.1 M with an electrolyte concentration of KH_2PO_4 of 0.1 M [PO_4] at temperature 37 ^oC were selected based on our earlier studies with the direct glucose AEMFC [6, 9]. Different anode catalysts such as Pt, PtRu, PtNi, Au and PdAu considered to be effective for the oxidation reaction of glucose [2, 10-11] were used in a membrane electrode assembly (MEA). Four of the anode catalysts had a total metal content of 40 wt.% supported on carbon, except for PtRu, which had the total metal content of 60 wt.%. Pt and PtNi were also used having 60 and 10 wt.%, respectively. As the cathode catalyst in all tests, carbon supported Pt with a total metal content of 60 wt.% was applied. For measuring the polarization curves and/or the Coulombic efficiency tests (i.e. stability tests), the in-house-made electrical load with a PI-controller (i.e. a feedback controller that has proportional and integral action on control error signal) for maintaining either constant current (CC) or constant voltage (CV mode) was used.

2. EXPERIMENTAL

2.1 The test equipment

2.1.1 Main device

The main device is shown in Fig. 1. This was made up of the plate type cell configuration (by Fuel Cell Technologies, USA) having a geometrical area of the electrodes of 5 cm^2. The flow channels on the surface of the anode graphite block in contact with the anode were widened in order to increase the flow of the fuel to the anode and operate at a moderate pressure. An anion exchange membrane (AEM, FAA-3-PP by Fumatech) was inserted between the electrodes. Preparation steps for the AEM were similar to our earlier report [6], except that the ion-exchange time for the membrane was decreased from 24 hours to only one hour. The torque of 5 Nm was used while pressing the anode and cathode together with bolts. The liquid was recirculated by a peristaltic pump (Watson Marlow 120) between the anode side of the fuel cell and the pumping tank (volume of 100 ml).

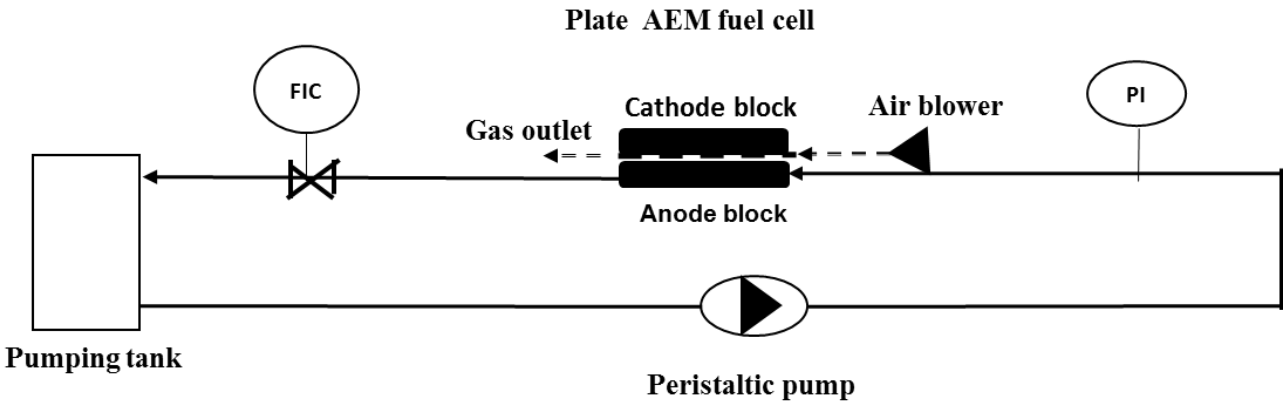

Figure 1. Main device of the fuel cell system.

The control of liquid flow was measured and controlled by a manual rotameter (FIC) ranging from 5.5 to 6 ml min^{-1}. The liquid pipeline included a pressure indicator (PI) before the fuel cell. The pressure of the fuel-electrolyte solution before the fuel cell varied between 1.1 bar and 1.6 bar during the test. The air was supplied to the cathode side of the fuel cell by a pc-blower. The electrical connections in the test fuel cell system are shown in Fig. 2.

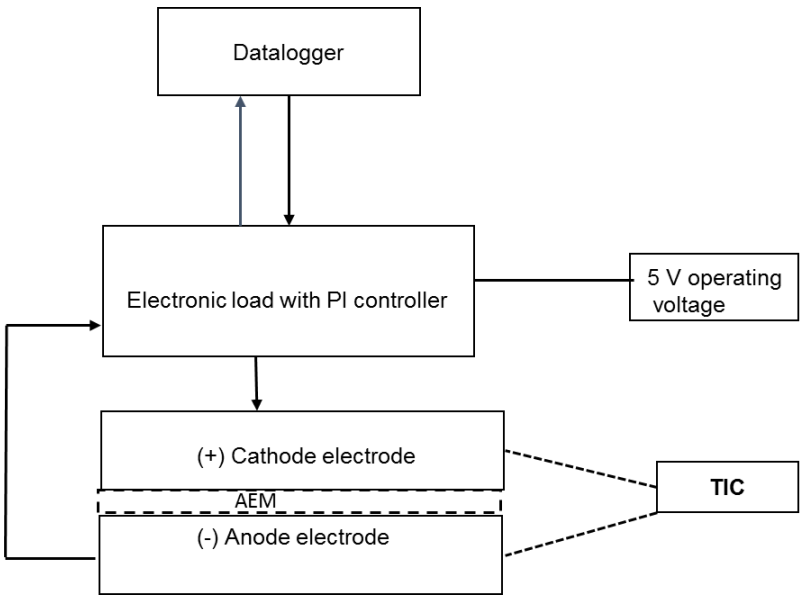

Figure 2. Electrical connection in the fuel cell system.

The electrodes of the test fuel cell were connected to the electronic load with a PI controller (ELPIC). 5 V operating voltage was used for the ELPIC. The temperatures of both the anode and cathode were controlled by a temperature controller (TIC) of the electric heating system. The current and voltage values were obtained by connecting to a PC with a data logger.

2.1.2 Preparation of the electrodes

The properties of the tested catalysts are listed in Table 1. Au(40 wt.%), PdAu(40 wt.%), PtNi(10 wt.%) and PtNi(40 wt.%) were manufactured by Premetek (Vulcan XC-72 as the carbon support) and Pt(40 wt.%), Pt(60 wt.%) and PtRu(60 wt.%) by Alfa Aesar (carbon black and activated carbon as the supports). The metal nanoparticle size for Au(40 wt.%), PdAu(40 wt.%), Pt(40 wt.%), Pt(60wt.%) and PtRu(60 wt.%) is around 3 nm while the PtNi nanoparticles are larger with sizes between 8-20 nm. These values were reported by the manufacturers.

The electrodes were prepared by a method developed for a FAA3-based direct methanol fuel cell (DMFC) as was reported earlier by Kanninen et al. [12]. Anode catalyst inks for glucose were prepared by first mixing the different carbon supported catalysts with 100 µl of water and 600 µl of isopropanol for 10 mins. FAA3 ionomer solution (12 wt.% in N-methyl-2-pyrrolidone, Fumatech GmbH) was added and the mixing continued for another 30 mins. The inks were subjected to 15 min of sonication and finally mixed by a magnetic stirrer overnight with the exception of the PtRu ink, which was only blended for 2 h due to precipitation if longer mixing was allowed. The resulting slurry was painted on a pre-weighted hydrophilic gas diffusion layer (GDL, ELAT-H, FuelCellEtc, thickness 300 µm) by a Badger 100-3-GF air brush and dried in a vacuum oven at 40°C for 2 h with the vacuum pump on for 30 min. The GDL was then weighed to determine the weight of the dry catalyst layer. The catalyst loadings of the anodes were between 1.2 and 1.6 mg cm^{-2} (see Table 1) and the FAA3 ionomer content was 30 wt.% of the whole dry mass of the anode as also reported in [13].

The cathodes for the MEAs were fabricated from a catalyst of Pt supported on high surface area carbon (60 wt.% Pt, Alfa Aesar) on a hydrophobic GDL (GDL-CT, FuelCellEtc, thickness 410 µm) by a similar method as the anodes. The Pt loadings were 2.7 ± 0.2 mg cm^{-2} and the FAA3 ionomer content was 30 wt.%. A higher loading and similar loadings at the cathode were used to ensure that the catalytic activity of the fuel cell would only be limited by the anode. The MEAs were not hot-pressed due to the sensitivity of the FAA3 membrane to pressure and temperature [13].

Table 1. The anode catalysts and their metallic mass loadings.

Anode catalyst (wt.%)	**Carbon support type**	**Manufacturer**	**Particle size (nm)**	**Total mass loading [mg cm^{-2}]**
Au (40)	Vulcan XC-72	Premetek	3-6	1.48
PdAu(1:1) (40)	Vulcan XC-72	Premetek	3-6	1.57
Pt (40)	carbon black	Alfa Aesar	3.4	1.50
Pt (60)	activated carbon	Alfa Aesar	2.8	1.37
PtNi(1:6) (10)	Vulcan XC-72	Premetek	8-20	1.20
PtNi(1:6) (40)	Vulcan XC-72	Premetek	8-20	1.49
PtRu(1:1) (60)	carbon black	Alfa Aesar	2.7	1.37

2.1.3. The gaskets of the test fuel cell

For the anode electrodes of under 500 μm thickness (i.e. Au (40%), Pt (40%), Pt (60%), PtNi (40%) and PtRu (60%)) nitrile rubber gaskets with a thickness of 350 μm were applied. Whereas for the cathode electrodes with Pt (60%) of 490 to 500 μm thicknesses PTFE - glass fiber gaskets with a thickness of 250 μm were used. For the anode electrodes of a thickness of equal or above 500 μm (i.e. PdAu (40%), PtNi (10%)), a rubber gaskets with thickness of 380 μm were inserted on the cathode side in addition to the PTFE gasket.

2.1.4 Electronic load with PI –controller (ELPI)

The electronic load had been built on a TeensyLC microprocessor board. The electronic load could run in either constant current or constant voltage modes. The control actuator was a transistor. The microprocessor controlled the base-emitter voltage by using a D/A (a digital analog converter inside a microcontroller chip) channel. The microprocessor read load voltage, load current and potentiometer voltage by using A/D (i.e. analog digital converter) channels from 0 to 2. The A/D channels 0, 1 and 2 read the voltage of the load current sensing resistor, the load voltage and the potentiometer voltage, respectively. The microprocessor was programmed by using Teensyduino IDE software. The voltage or current set point was given by the operator by using the potentiometer. The 32 bit microcomputer run a PI-control algorithm that computes the transistor base-emitter voltage. The current was measured by a 10 ohm shunt resistor between the transistor base and system ground.

2.2. The test procedure

The test procedures were similar to our earlier work [6, 9]. Glucose and potassium dihydrogen phosphate (KH_2PO_4 ,Sigma-Aldrich] were dissolved in distilled water. The concentrations of glucose and of KH_2PO_4 were 0.1 M. The pH value of each solution was set at a value of 7.4 by adding potassium hydroxide (KOH, Algol) in the aqueous solution of both glucose and KH_2PO_4.

The fuel - electrolyte solution was pumped to the anode, in which the plates were electrically heated and maintained at temperature of 37 ^oC by the TIC controller. The open circuit voltage (OCV) generation was recorded until a steady-state or minimal variation of 50 $\mu V\ min^{-1}$ was obtained. After this step, the polarization curve was recorded until the voltage of the fuel cell fell decreased to values around 100 mV by varying the current value by the electronic load (using constant current (CC) mode of the electronic load). Following the polarization curve, the Coulombic efficiency over time (i.e. the stability tests) was recorded as follows: At the start the current values were set by the PI-controller (in constant voltage (CV) mode) of the electronic load to values in order between 25 to 40 % of the maximum current value of the maximum current density for each anode-cathode pair (i.e. current values between 100 and 800 μA). After 16 hours, except for PtRu and Pt (40 wt.%) as anodes, from the beginning of each test period, the voltage of the fuel cell was set in values near 100 mV until the current decreased down to a value between 20 and 30 μA. For anodes containing Pt (40 wt.%) and PtRu, the voltage was set to a value of 100 mV after four and 5.5 hours, respectively. The Coulombic

Efficiencies (CE, %) based on the two electron transfer and the specific energy value (SPEC, Wh kg $^{-1}$ glucose) were calculated similarly as to earlier reports [6, 9]. While measuring the Coulombic efficiency, the heating of the cell to 37 ^{o}C caused minor evaporation of water although water vapor was fed to the suction side of the pc-blower. The evaporation rate was found to be 0.50 ml /h. In order to avoid the effect of evaporation on the total concentration of the aqueous electrolyte, distilled water was added in the pumping tank as regularly as possible.

3. RESULTS AND DISCUSSION

3.1 Polarization curves

Table 2 shows the OCV values and the maximum current densities obtained from the cell combinations having different anode electrocatalysts with the cathode, except for PdAu and PtNi (both 40 wt.%). Table 2 shows also the ratios of the maximum current densities to the total catalyst loading in each anode (Table 1).With PdAu and PtNi (40 wt.%) as the anode electrocatalysts, the fuel cell did not generate any effective OCV values. The polarization tests were repeated twice with separate electrodes for both the PdAu (40 wt.%) and PtNi (40 wt.%) anode catalysts in the fuel cell without any improvements in the obtained OCV values as shown in Table 2.

Table 2. The polarization data of the fuel cell with different anode electrodes and ratios of current density value to total catalyst loading for each anode (Table 1). Pt (60%) as the electro catalyst in the cathode electrodes.

Anode catalyst (wt.%)	OCV [mV]	Maximum current density before 0.1 V [mA cm^{-2}]	Current density / total metallic mass density in anode electrode [A g^{-1}]
Au (40)	250	0.15	0.10
PdAu (40)	12	(not available)	(not available)
Pt (40)	275	0.13	0.09
Pt (60)	605	0.70	0.51
PtNi (10)	420	0.24	0.20
PtNi (40)	140	(not available)	(not available)
PtRu (40)	221	0.12	0.09

The polarization curves for the performing catalysts (i.e. Au (40%), Pt (40%), Pt (60%), PtNi (10%) and PtRu (40%)) as the anode are shown in Fig. 3. The maximum values for the current[SJ1] density (in Table 2 and Figure 3) corresponded the voltage values much higher than 100 mV, which was the final voltage of the fuel cell in our earlier studies with the cylinder-type AEMFC [6, 9]. The Figure 3 shows that a linear relationship between small current densities and voltages is valid (e.g. at current densities under 0.45 mA cm^{-2} with Pt (60%) as the anode catalyst). At higher current densities

(e.g. above 0.45 mA cm^{-2} with Pt (60%) as the anode catalyst) the mass transfer limitations (i.e. deviation from the linear polarization) take place. The low scale oxidation at high currents could also be explained by the catalyst being poisoned by the intermediate products of glucose oxidation [14]. The voltage values, which corresponded to maximum current density values (Table 2) for each anode electrocatalyst material, are collected and shown in Table 3.

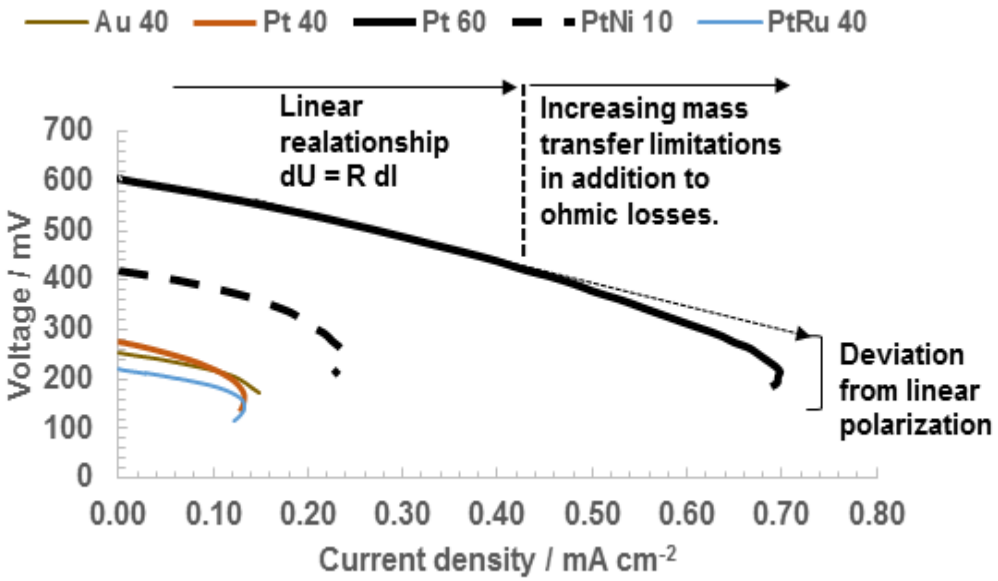

Figure 3. The polarization curve for the direct glucose AEMFC with the performing anode catalysts with Pt (60%) at the cathode electrocatalyst at 37 oC . Linear and unlinear regions of the polarization curve, when Pt(60) as the anode catalyst was applied, are shown.

Table 3. The voltage values corresponding the maximum current densities (Table 2) for each anode catalyst material.

Anode catalyst (wt.%)	**The voltage value corresponding the maximum current density [mV]**
Au (40)	170
PdAu (40)	(not available)
Pt (40)	153
Pt (60)	220
PtNi (10)	250
PtNi (40)	(not available)
PtRu (40)	150

From Table 2 it is observed that the two best anode electrocatalysts among the different types of anode materials were Pt (60wt.%) and PtNi (10 wt.%), obtained by the current-voltage characterizations. The anode electrocatalysts of PtNi (10 and 40 wt.%) were not of the Raney-type used by Richter et al [2]. However, among these two electrocatalysts PtNi (10 wt.%) shows higher

activity than PtNi (40 wt.%), implying that the later may have higher aggregation of catalyst particles and therefore reduced surface area available for glucose oxidation. All the catalysts with 40 wt.% total content showed much lower OCV values when compared to those two high performing anodes.

When the total thicknesses of the PtNi (10 and 40 wt.%) anodes were compared, PtNi (10wt.%) with the thickness of 700 μm enabled better results than PtNi (40 wt.%) with the thickness of 460 μm although the ohmic and mass transport losses should be higher with the electrodes with the higher thicknesses. Obviously the thicker catalyst layer made from PtNi (10 wt.%) produced more effective active area for glucose oxidation reactions. This could be due to more access to the catalyst sites and thereby increasing the possibility of further reactions by enhancing the current output and fuel efficiency. However, the optimization of the catalyst layer structure is out of the scope of this work and will be performed in future works. The particle sizes of the catalysts (shown in Table 1 as given by the manufacturers) were about 2.8 nm for Pt (60%) and in the range between of 8 to 20 nm for PtNi (10 and 40 wt.%). According to the manufacturer Premetek, the particle sizes of PtNi increases with the total content of the metal in the catalyst meaning that there is more active surface area available in PtNi (10 wt.%) catalyst. This could partly explain the performance difference between PtNi (10 wt.%) and PtNi(40 wt.%). Also, the smaller particle size of Pt (60 wt.%) when compared to PtNi explains its good performance in the fuel cell tests (Tables 2).

The poor performance of the AuPd(40 wt.%) and PtRu(60 wt.%) are most likely due to ineffectiveness of these catalysts for glucose oxidation in near-neutral-state aqueous electrolytes in contact with the AEM. The electrolyte containing phosphate anions neutralizes also the membrane and decreases its pH closer to neutral. The good performances of AuPd and PtRu have been previously published in alkaline and acidic conditions [10]. Even in a high performance alkaline direct glucose fuel cell using PtRu at the anode [11], the performance without aqueous electrolyte NaOH (in other words, close to neutral) remained very low indicating that PtRu may not work well in neutral conditions. For PtNi(40 wt.%), the poor OCV is difficult to explain but has most likely to do with the electrode structure as PtNi(10%) provided high OCV. It could be that the surface properties of the catalyst exclude glucose from the catalyst layer thus decreasing the OCV. Au has been reported as an efficient catalyst for glucose oxidation in both alkaline and neutral [15-17] but Au(40 wt.%) did not perform very well in these fuel cell tests. This could be due to the Au/C catalyst used here instead of bulk Au used in previous studies in near-neutral conditions [15, 17].

The conductivity of the fuel cell system is reduced compared to acidic and alkaline systems due to the phosphate salts in the near-neutral-state electrolyte as they have lower conductivity than the small protons and hydroxide ions. Moreover, the ionic conductivities of the AEM materials are reported to be lower in the presence of different aqueous salts and their ions (i.e. PO_4^{3-}, HCO_3^- and CO_3^{2-}) compared to hydroxide [18]. This would imply that the main current carrier becomes multi-charged anions thus increasing the membrane resistance [18]. The reduction in conductivity in combination with the reduced catalytic activity near neutral pH implies that the near-neutral-state direct glucose fuel cells may not reach similar current density values than the direct glucose fuel cells operating in alkaline environments [2, 6-8, 19].

Comparing the performance of direct glucose AEMFC to other AEMFC systems using different fuels like hydrogen and methanol reveals a further limitation. When the ratios of current

densities to catalyst loading for each anode (Table 2) are taken into account, the values are obviously distinctly lower compared to e.g. 700 A g^{-1}, which was attained with the composite AEM H_2 / air fuel cell [20]. The corresponding values for alkaline direct methanol AEMFC with and without aqueous alkaline electrolyte are 22 and 2.6 A g^{-1}, respectively [21-22]. Even though that the systems in reported studies are not totally similar, it seems that it is not feasible to increase the current densities of glucose fuel cells as high as those of H_2 or even methanol fuel cells due to the slow kinetics of glucose oxidation but improvements can be made with the optimization of the catalyst and the MEA. Therefore, direct glucose AEMFC is intended for the applications in small power supplies in portable electric devices and/or as an electric charger for batteries instead of power plant or high power applications [6].

3.2 Coulombic efficiency

The results from Coulombic efficiency tests with the AEMFC are shown in Table 4. Coulombs were measured until the voltage of the AEMFC reached the voltage value of 100 mV and current values between 20 and 30 μA. Average voltage values were obtained and respective values of the specific energy and Coulombic efficiency (based on 2e- transfer) were calculated. The Coulombic efficiency could not be measured for PdAu and PtNi (40 wt.%) as anodes due to the very low OCV values (Table 2). The AEMFCs based on glucose as a fuel with anode catalysts Pt (60 wt.%) and PtNi (10 wt.%) show high specific energies and Coulombic efficiencies having high initial OCVs between 600 and 400 mV (Table 2).

Table 4. Measured and calculated data of the direct glucose AEMFC with different anode.

Anode catalyst (wt.%)	**Measured Coulombs ∑ As**	**Average voltage [mV]**	**Average power [mWh]**	**Specific energy [Wh kg^{-1}]**	**Coulombic efficiency [%/ 2 e-]**
Au (40)	4.59	124	0.16	0.088	0.24
PdAu (40)	-	-	-	-	-
Pt(40)	1.39	119	0.046	0.025	0.07
Pt (60)	24.80	126	0.87	0.48	1.30
PtNi (10)	10.37	112	0.34	0.19	0.54
PtNi (40)	-	-	-	-	-
PtRu (40)	3.20	92	0.082	0.05	0.17

The recorded current[SJ2]-voltage values as function of time for the tested AEMFC with Pt (60 wt.%) in the anode as the best electrocatalyst are shown in Fig. 4. The results (presented in Table 4 and Fig. 4) show that the overall Coulombic efficiency values together with the measured current densities remained very low when compared to earlier reports [2-3]. The results also show that these values are far lower than those reported having a cylinder-type AEMFC with glucose as fuel in

the near-neutral-state electrolyte [6, 9]. The influences of the differences in the electrodes design on the performances of the fuel cells have been earlier reported with the polymer electrolyte fuel cell (PEMFC) and the membraneless microfluid fuel cell [23, 24] with hydrogen gas and formic acid as fuels, respectively. The previous is suggested to be valid also when the differences between the direct plate and cylinder glucose fuel cells are taken into account.

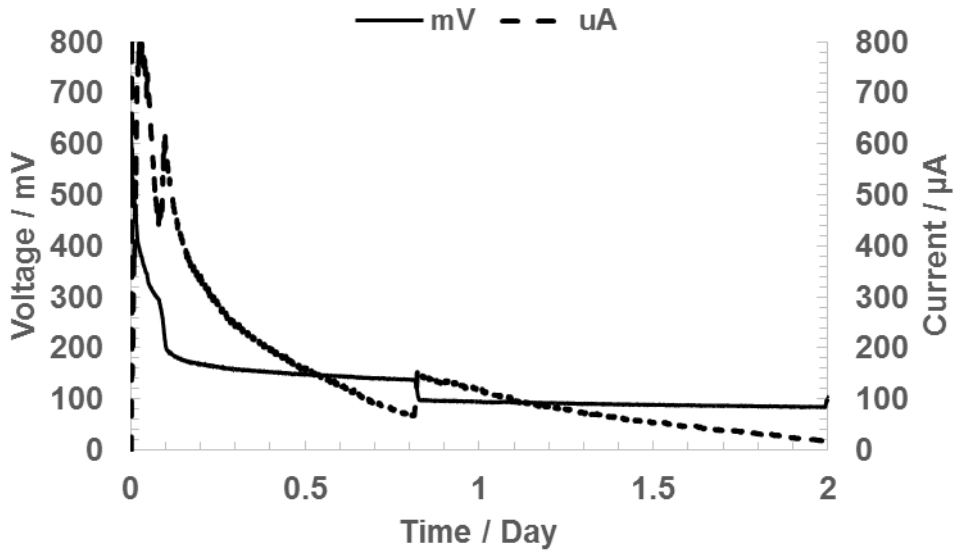

Figure 4. The recorded current-voltage values with a combination of the best Pt (60 wt.%) anode and Pt (60wt.%) cathode electrodes. The left y-axis is for the voltage and the right y-axis is for the current.

The commercial electrical loads are mainly used for the order of magnitude of ampere (A) currents causing high relative errors when applied to low current, which we were to utilize and construct our own electronic load for measuring small currents. Use of in-house-made electronic load with PI controller (ELPIC), does imply a slight leakage current during the first test in the voltage of the AEMFC (e.g. PtRu as an anode) from the set value for the voltage (100 mV) down to the values between 90 and 100 mV with the low currents of 70 µA. The voltage value of the AEMFC was monitored on the screen of pc, which was in contact with the data logger. However after fine tuning of the parameters of the PI controller, the control accuracy was improved so that the final voltage of 100 mV was maintained in the range of 98 to 100 mV. On the whole, the use of the in-house-made ELPIC is acceptable for validating our results in this study. In the future the research directions will include the selection of the operation values (voltages, current densities, electrode designs) of the direct glucose AEMFCs together with further development in the control system and methods. The electronic load with the PID controller (i.e. the controller that includes additional derivative action on control error signal) is assumed to be necessary for maintaining the precise setting values for the control of voltage of the fuel cell.

4. CONCLUSIONS

In this work five different anode electrocatalysts were tested with the similar Pt cathodes. Based on the obtained and calculated results (specific energy (SPEC) and Coulombic efficiency (CE) values), Pt (60 wt.%) and PtNi(10 wt.%) were found to be the most effective anode electrocatalyst materials from all the studied materials in this work. These catalyst were selected to be used in future fuel cell tests. The in-house-made electronic load with a PI controller was applied to low currents, and its operation was acceptable for validating our results in this study. Improvement in performance should be viable through electrode structure optimization, which will be done in future works together with the optimization of the direct glucose AEMFC operation. Also the further development of the electronic load with a PI or PID controller will be necessary for maintaining precise setting values for the control of voltage of the fuel cell.

ACNOWLEDGEMENTS
This research was financially supported by Jane & Aatos Erkko Foundation.

References

1. J.-P. Spets, M. Kuosa, T. Granström, Y. Kiros, J. Rantanen, M. J. Lampinen, K. Saari, *Mater Sci Forum*, 638-642 (2010) 1164.
2. U. Gebhardt, J. R. Rao, G. J. Richter, *J Appl Electrochem*, 6 (1976) 127.
3. J. R. Rao, G.J. Richter, *Naturwissenschaften*, 61 (1974) 200.
4. S. Kerzenmacher, J. Ducrée, R Zengerle, F. von Stetten, *J Power Sources*, 182 (2008) 66.
5. D. H. Park, J. G . Zeikus, *Appl Environ Microb*, 66 (2000) 1292.
6. J.-P. Spets, M. J. Lampinen, Y. Kiros , J. Rantanen, T. Anttila, *Int J Electrochem Sci*., 7 (2012) 11696.
7. J-P. Spets, M. J. Lampinen, Y. Kiros, T. Anttila, J. Rantanen, T. Granström, *Int J Electrochem Sci*., 5 (2010) 547.
8. E. Katz, *Electroanal*, 22(2010) 744.
9. J.-P. Spets, M. J. Lampinen, Y. Kiros, J. Rantanen, T. Anttila, *Int J Electrochem Sci*., 8 (2013) 1226.
10. A. Brouzgou, P. Tsiakaras, *Top Catal*, 58 (2015) 1311-1327.
11. N.Fujiwara, S.-i. Yamazaki, Z. Siroma,T. Ioroi, H.Senoh, K. Yasuda. *Electrochem Commun*, 11 (2009) 390.
12. P. Kanninen, M. Borghei, O. Sorsa, E. Pohjalainen, E. I. Kauppinen, V. Ruiz, T. Kallio, *Appl Cat B: Environ*, 156-157 (2014) 341.
13. M. Carmo, G. Doubek, R.C. Sekol, M. Linardi, A.D. Taylor, *J Power Sources*, 230 (2013) 169.
14. C. A. Apblett, D. Ingersoll, S. Sarangapani, M. Kelly, P. Atanassov, *J Electrochem Soc*, 157 (2010) B86.
15. K.B. Kokoh, J.-M. Léger, B. Beden, C. Lamy, *Electrochim Acta* 37 (1992) 1333.
16. M. Guerra-Balcázar, D. Morales-Acosta, F. Castaneda, J. Ledesma-Carcía, L. G. Arriaga, *Electrochem Commun*, 12 (2010) 864.
17. M Wooten, J. H. Shim, W. Gorski, *Electroanal*, 22(2010) 1275.
18. N. Pismenskaya, V. Nikonenko, B. Auclair, G. Pourcelly, *J Membrane Sci*., 189 (2001) 129.
19. J.-P. Spets, Y. Kiros, M.A. Kuosa, J. Rantanen, M. J. Lampinen, K. Saari, *Electrochim Acta* 55 (2010) 7706.

20. E. Hao Yu, X. Wang, U. Krewer, L. Li, K. Scott, Energ *Environ Sci.*, 5 (2012) 5668.
21. A. Santasalo-Aarnio, S. Hietala, T. Rauhala, T. Kallio, *J Power Sources*, 196 (2011) 6153.
22. C. Coutanceau, L. Demarconnay, C. Lamy, J.-M. Léger, *J Power Sources*, 156 (2006) 14.
23. R. A. García-Cuevas, I. Cervantes, L. G. Arriaga, I. A. Diaz-Diaz, *Int J Hydrogen Energ*, 38 (2013) 14791.
24. J.-F. Coursange, A.Hourri, J.Hamelin, *Fuel Cells*, 3 (2003) 28.